euspen's 20th International Conference & Exhibition, Geneva, CH, June 2020
www.euspen.eu

Effect of oil film thickness on motion errors for closed hydrostatic guideway with four pads

Chenchun Shi, Yunfeng Peng*, Zhenzhong Wang, Ping Yang, Guo Bi, Wei Yang, Chenlei Li

Department of Mechanical and Electrical Engineering, Xiamen University, Xiamen 361005, China

pengyf@xmu.edu.cn

Abstract
Hydrostatic guideways are widely applied as the vital functional unit in precision and ultra-precision machine tools owing to their low running friction, high stiffness, high motion accuracy, etc. Since the motion errors of hydrostatic guideways directly affect the accuracy of the machined parts, there have been many researches concerning the motion accuracy of hydrostatic guideways. However, it seems that the influence of oil film thickness (OFT) on motion errors in closed hydrostatic guideways has not been thoroughly studied yet. Different from those previous approaches, the quasi-static analysis model with less simplification is directly developed by incorporating the concept of pose in this paper, which is then employed to explore the effect of OFT on motion accuracy in the field of hydrostatic guideways. The typical closed hydrostatic guideway with four pads is still adopted as the sample here. The numerical results demonstrate that, OFT hardly affects the motion errors if the external force acting on the hydrostatic table is not considered, whereas the effect does occur if the external force is taken into account. Further, the mechanism of motion errors variation is attributed to the fluctuation of the difference between the average film thicknesses of the two adjacent pads, the greater the fluctuation, the larger the motion errors.

Oil film thickness; Motion error; Hydrostatic guideway; Guide rail; Pose; Oil pad

1. Introduction

Hydrostatic guideways have been widely applied as the vital functional unit in precision and ultraprecision machine tools for their low running friction, high stiffness, high motion accuracy, superior vibration-resistance, virtually no wear, long service life, etc [1-5]. Due to that the motion errors of hydrostatic guideways affect the accuracy of the machined parts directly, quite a few researches related to the motion accuracy of hydrostatic guideways were carried out. However, it seems that the influence of oil film thickness (OFT) on motion errors in closed hydrostatic guideways has not been thoroughly studied yet.

In this paper, the typical closed hydrostatic guideway with four pads is taken as the sample, which also is commonly used in other researches [5-7]. Besides, different from the previous approaches including the transfer function method (TFM) [8], the simplification of oil film as the linear spring element [5, 9] and finite element analysis (FEA) [10], the quasi-static analysis model with less simplification is directly developed by incorporating the concept of pose, which is then employed to explore the effect of OFT on motion accuracy in the field of hydrostatic guideways. Our research is expected to be inspiring to the designers, and some theoretical references for precision design of hydrostatic guideways can be drawn.

2. Quasi-static analysis model

Figure 1 shows the typical closed hydrostatic guideway with four pads. The OFT proposed in our study does refer to the sum of h_{01} and h_{02}, as seen in Figure 1 (a), it also can be considered as the designed total oil film clearance. Additionally, {*A*} is introduced as the reference coordinate system, and the distance between ideal rail 1 (2) and the plane $o_A x_A y_A$ is $h_0/2$. Then, {*B*} is determined as the hydrostatic table coordinate system, as depicted in Figure 1 (b). Figure 1 (c) exhibits the structure of every rectangular pad.

As observed from Figure 1 (a), the linear motion error z_A and angular motion error ϑ do exist because of the real guide rails 1 and 2 with profile errors. They can be expressed as [5-6, 9]

$$Z_1 = E_1 \sin\left[\frac{2\pi}{\lambda_1}\cdot\left(X-\frac{L}{2}\right)+\varphi_1\right]-\frac{h_0}{2} \quad (1)$$

$$Z_2 = E_2 \sin\left[\frac{2\pi}{\lambda_2}\cdot\left(X-\frac{L}{2}\right)+\varphi_2\right]+\frac{h_0}{2} \quad (2)$$

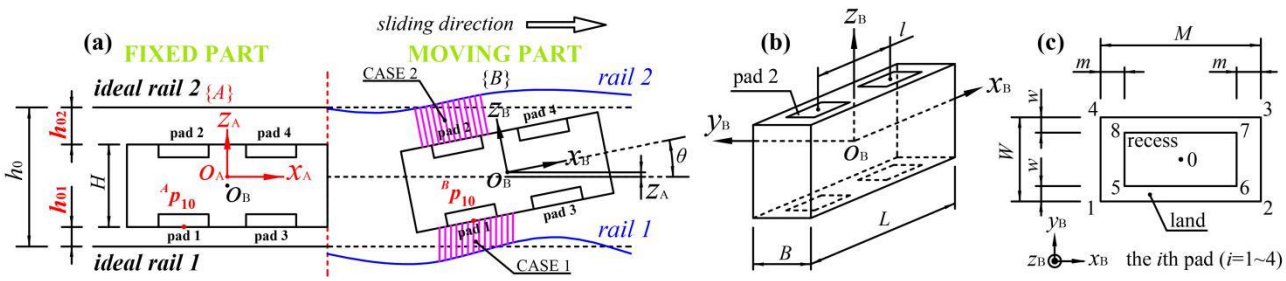

Figure 1. Typical closed hydrostatic guideway with four pads (a) pose of hydrostatic table, (b) structure of hydrostatic table, and (c) rectangular pad

Where E_1, E_2, λ_1, λ_2, φ_1, φ_2 denote the profile error amplitude, wavelength and phase of guide rails 1 and 2, respectively. The quasi-static analysis model then is developed based on the static equilibrium. Both the resultant force and resultant moment of the hydrostatic table must equal to zero wherever it moves [4-5, 9]. As shown in Figure. 2, the force and the moment equilibrium equations are expressed as

$$F_{4u}+F_{2u}+F_0=F_{1u}+F_{3u}\Rightarrow \quad F_4\cos\theta+F_2\cos\theta+F_0=F_1\cos\theta+F_3\cos\theta \tag{3}$$

$$M_{O_BY_B}=0\Rightarrow F_0\cdot e+F_4\cdot\frac{l}{2}+F_1\cdot\frac{l}{2}=F_2\cdot\frac{l}{2}+F_3\cdot\frac{l}{2} \tag{4}$$

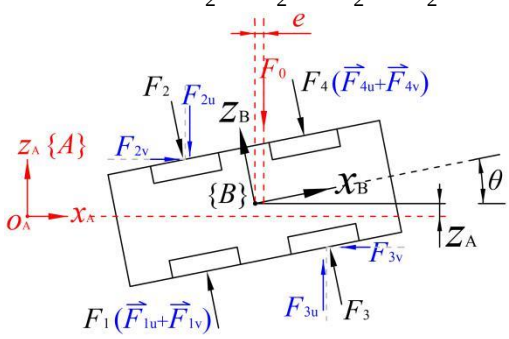

Figure 2. Static equilibrium of hydrostatic table with four pads

By solving the Eqs. (3) and (4), the two motion errors can be determined. Hence, the oil film reaction force F_i (i=1~4) needs to be obtained first, the expression of F_i is given as [11]

$$F_i\left(i=1\sim4\right)=P_{ri}\cdot A_{ei} \tag{5}$$

Here, P_{ri} is the hydrostatic pressure in the recess. A_{ei} is the effective bearing area of the rectangle pad, it can be written as

$$A_{ei}\left(i=1\sim4\right)=\left(W-w\right)\cdot\left(M-m\right) \tag{6}$$

Note that, the progressive mengen (PM) flow controllers are adopted in the closed hydrostatic guideway shown in Figure 1. PM controller is the product of Hyprostatik Company in Germany and belongs to the membrane-type restrictor, which has been widely used as the key component in other precision machine tools [12-14]. Its structure and working principle can be easily found in [12, 15]. So P_{ri} can be calculated by

$$\underset{(i=1\sim4)}{P_{ri}}=\frac{Q_0\cdot R\left(h_{ai}\right)}{1-\dfrac{Q_0\cdot\left(K_r-1\right)}{P_s}\cdot R\left(h_{ai}\right)} \tag{7}$$

where Q_0 is the initial flow rate for P_r=0, K_r is named as flow ratio, P_s is the supply pressure. They are regarded as the three key characteristic parameters of PM controller. Besides, $R(h_{ai})$ is the flow resistance of the land and related to the average oil film thickness h_a [4, 9]. $R(h_{ai})$ can be obtained as

$$\underset{(i=1\sim4)}{R\left(h_{ai}\right)}=\frac{3\eta}{h_{ai}^{\ 3}\cdot\left(\dfrac{M-m}{4w}+\dfrac{W-w}{4m}\right)} \tag{8}$$

Lastly, the calculation of h_{ai} is essential. As seen in Figure 1 (a), CASE 2 is chosen to determine the h_{ai} and it is given as

$$h_{a1}=\frac{1}{A_{land}}\cdot\left(\begin{array}{l}\int_{{}^Ap_{11y}}^{{}^Ap_{14y}}\mathrm{d}Y\int_{{}^Ap_{11x}}^{{}^Ap_{12x}}\left(Z_{13}-Z_1\right)\mathrm{d}X\\-\int_{{}^Ap_{15y}}^{{}^Ap_{18y}}\mathrm{d}Y\int_{{}^Ap_{15x}}^{{}^Ap_{16x}}\left(Z_{13}-Z_1\right)\mathrm{d}X\end{array}\right) \tag{9}$$

$$h_{a3}=\frac{1}{A_{land}}\cdot\left(\begin{array}{l}\int_{{}^Ap_{31y}}^{{}^Ap_{34y}}\mathrm{d}Y\int_{{}^Ap_{31x}}^{{}^Ap_{32x}}\left(Z_{13}-Z_1\right)\mathrm{d}X\\-\int_{{}^Ap_{35y}}^{{}^Ap_{38y}}\mathrm{d}Y\int_{{}^Ap_{35x}}^{{}^Ap_{36x}}\left(Z_{13}-Z_1\right)\mathrm{d}X\end{array}\right) \tag{10}$$

$$h_{a2}=\frac{1}{A_{land}}\cdot\left(\begin{array}{l}\int_{{}^Ap_{21y}}^{{}^Ap_{24y}}\mathrm{d}Y\int_{{}^Ap_{21x}}^{{}^Ap_{22x}}\left(Z_2-Z_{24}\right)\mathrm{d}X\\-\int_{{}^Ap_{25y}}^{{}^Ap_{28y}}\mathrm{d}Y\int_{{}^Ap_{25x}}^{{}^Ap_{26x}}\left(Z_2-Z_{24}\right)\mathrm{d}X\end{array}\right) \tag{11}$$

$$h_{a4}=\frac{1}{A_{land}}\cdot\left(\begin{array}{l}\int_{{}^Ap_{41y}}^{{}^Ap_{44y}}\mathrm{d}Y\int_{{}^Ap_{41x}}^{{}^Ap_{42x}}\left(Z_2-Z_{24}\right)\mathrm{d}X\\-\int_{{}^Ap_{45y}}^{{}^Ap_{48y}}\mathrm{d}Y\int_{{}^Ap_{45x}}^{{}^Ap_{46x}}\left(Z_2-Z_{24}\right)\mathrm{d}X\end{array}\right) \tag{12}$$

where i denotes the number of pad, and j denotes the number of point in one pad plane. Based on the example depicted in Figure 1, i ranges from 1 to 4 and j from 0 to 8. The descriptions of point $\boldsymbol{q}$ on the hydrostatic table in {A} and {B} are different and denoted by ${}^A\boldsymbol{q}$ and ${}^B\boldsymbol{q}$, respectively. ${}^A\boldsymbol{q}_{ij}$ and ${}^B\boldsymbol{q}_{ij}$ are the coordinates of the jth point of the ith pad plane in {A} and {B}, respectively. A_{land} denotes the projected area of land in the plane $o_Ax_Ay_A$, it is

$$A_{land}=2w\left({}^Ap_{12x}-{}^Ap_{11x}\right)+2\left(W-2w\right)\left({}^Ap_{12x}-{}^Ap_{16x}\right) \tag{13}$$

Besides, pad 1 and pad 3 are in the same plane, and the corresponding mathematical equation can be denoted by Z_{13}, so is Z_{24}. Therefore, Z_{13} and Z_{24} can be expressed as

$$Z_{13}=-\tan\theta\cdot X+\tan\theta\cdot{}^Ap_{10x}+{}^Ap_{10z} \tag{14}$$

$$Z_{24}=-\tan\theta\cdot X+\tan\theta\cdot{}^Ap_{20x}+{}^Ap_{20z} \tag{15}$$

The relationship between the four oil film reaction forces and the two motion errors can be summarized as follow: Oil film reaction force F_i → Hydrostatic pressure in the recess P_{ri} → Flow resistance of the land R (h_{ai}) → Average oil film thickness h_{ai} → Motion position of the hydrostatic table and the motion errors (x_A, z_A, ϑ). Up to now, the establishment of the quasi-static analysis model has been completed.

3. Results and discussion

Three case studies are selected to investigate the effect of OFT on motion errors for closed hydrostatic guideway with four pads. The simulation condition has been listed in Table 1.

Table 1 Simulation condition of the typical closed hydrostatic guideway with four pads

Parameter	Hydrostatic table [6]			Rail 1
	l	L	H	E_1
Value	60.5 mm	125 mm	320 mm	4 μm
Parameter	Pad [6]			
	M	m	W	w
Value	60.5 mm	15 mm	50 mm	15 mm
Parameter	PM controller			Rail 1
	Q_0	K_r	P_s	λ_1
Value	1×10^{-7} m^3/s	1.4	5 MPa	280 mm
Parameter	Rail 2			Rail 1
	E_2	λ_2	φ_2	φ_1
Value	2 μm	140 mm	0.6π	0
Parameter	Stroke (mm)	Hydrostatic oil dynamic viscosity [6]		
		η		
Value	125 ~ 700	0.065 Pa·s		

3.1. Case study one

Case study one means that both the external force F_0 and its arm e shown in Figure 2 are set as zero. As can be observed in Figure 3 (a) and (b), the influence of OFT on the two motion errors are not significant at all, and the PV values of the two motion errors are also unchanged with the variation of OFT, as depicted in Figure 3 (c). However, it can be seen that the angular

and liner motion errors fluctuate periodically with the moving of hydrostatic table along the positive direction of x_A axis. Here, the horizontal axis named travel appears in Figures 3, 4 and 5, and it is just the x_A axis seen in Figure 1.

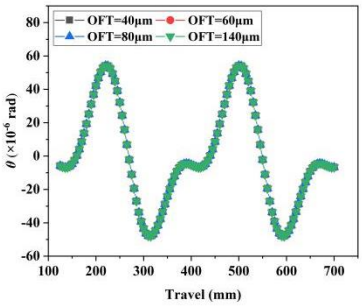

(a) angular motion error

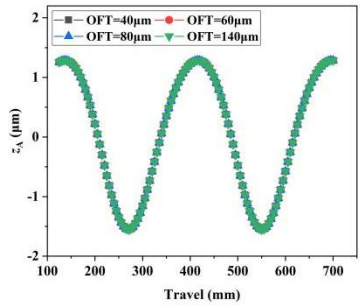

(b) linear motion error

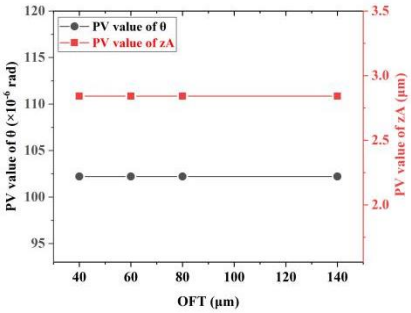

(c) PV values of the two motion errors

Figure 3. Influence of OFT on motion accuracy in case study one

3.2. Case study two

Case study two refers to that the external force F_0 is set as 1500 N, but its arm e is still zero. Figure 4 shows the influence of OFT on motion accuracy in case study two. As seen in Figure 4 (a), with the increase of OFT, the peaks of the angular motion error curve move along the negative direction of x_A axis, but the valleys move inversely. In Figure 4 (b), the peaks and valleys of these linear motion error curves are correspondent to each other, whereas the curve moves down with the growth of OFT, in other words, the hydrostatic table shown in Figure 1 (a) gets closer to the guide rail 1 along the positive direction of F_0. The two motion errors still fluctuate periodically. Additionally, the PV values of the two motion errors do rise with the increase of OFT, as depicted in Figure 4 (c), and they two change similarly.

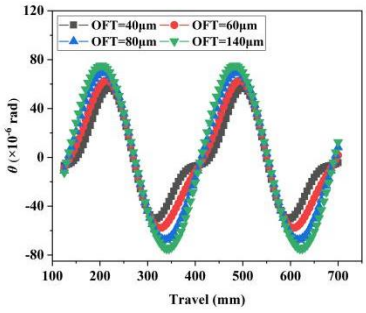

(a) angular motion error

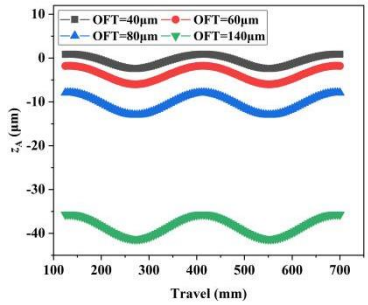

(b) linear motion error

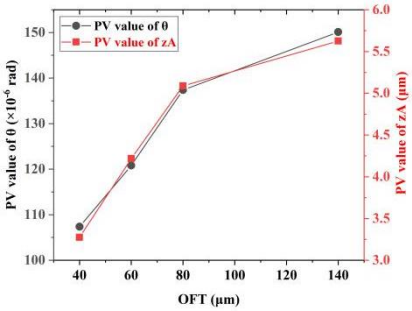

(c) PV values of the two motion errors

Figure 4. Influence of OFT on motion accuracy in case study two

3.3. Case study three

Case study three implies 1500 N of F_0 and 12.10 mm (0.2*l) of e. The two motion errors change periodically with the moving of hydrostatic table, as shown in Figure 5 (a) and (b). Moreover, with the increase of OFT, the peaks of the angular motion error curve move along the negative direction of x_A axis, but the valleys move inversely, which is similar to the phenomenon exhibited in Figure 4 (a), but the difference also is noticeable, the angular motion error curve moves up. The information presented from Figure 5 (b) and (c) is similar to that from Figure 4 (b) and (c). Accordingly, the arm e can affect the variation of the angular motion error significantly by comparing to case study two.

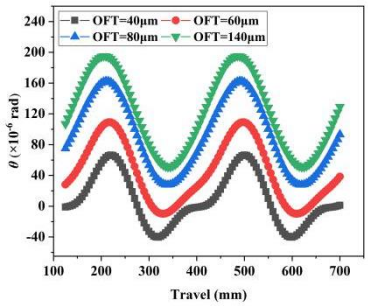

(a) angular motion error

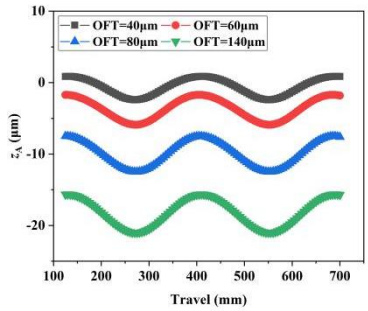

(b) linear motion error

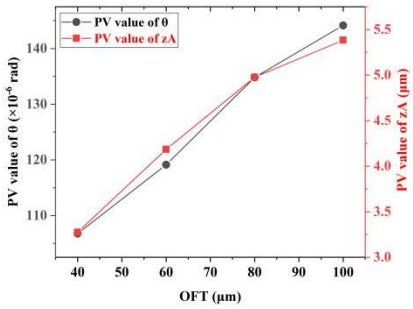

(c) PV values of the two motion errors

Figure 5. Influence of OFT on motion accuracy in case study three

3.4. Discussion

The numerical results shown in Figures 3, 4 and 5 suggest that, OFT hardly affects the motion errors if the external force acting on the hydrostatic table is not considered, whereas the effect does occur if the external force is taken into account. The mechanisms affecting motion accuracy are given further. It can be known that the motion errors were linked to the oil film reaction forces on the pads [5, 10]. However, as illustrated in the last part of Section 2, the oil film reaction force is related to h_a tightly.

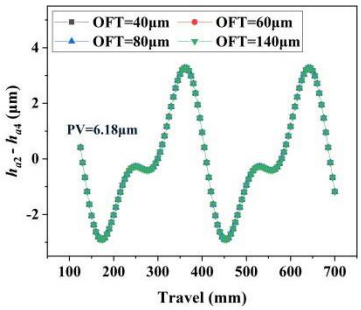

(a) Case study one

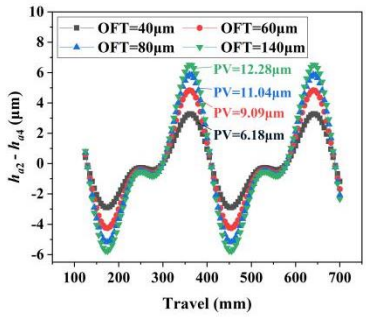

(b) Case study two

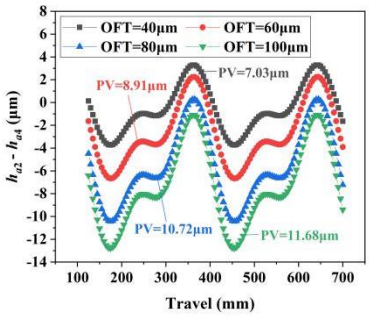

(c) Case study three

Figure 6. Variation of ρ with the change of OFT

In case study one, F_0 is not considered, so it is F_1=F_2 and F_3=F_4 that always holds, and there will always be h_{a1}=h_{a2} and h_{a3}=h_{a4}. Then, the difference between the average film thicknesses of two adjacent pads (such as pad 2 and 4 shown in Fig. 1) is named as ρ, which is mathematically expressed as ρ=h_{a2}-h_{a4}. It may be naturally inferred that, the greater the fluctuation of ρ, the larger the motion errors. Just as shown in Figure 6 (a), no matter how the OFT changes, ρ and its PV value are unaffected, which can interpret the phenomena shown in Figure 3. Does the explanation still work to the case studies two and three? As depicted in Figure 6 (b) and (c), the PV value of ρ rises with the increase of OFT, which corresponds to the results shown in Figure 4 (c) and Figure 5 (c), respectively. So the variation of the motion errors can almost be figured out now. The research work [16] also is suggested to be referred due to the similarity with this study, but the themes are different with each other.

4. Conclusions

The influence of oil film thickness on motion errors for closed hydrostatic guideway with four pads does exist, but the effect can be ignored if the external force is not taken in account. Besides, the parameter ρ (=h_{a2}-h_{a4}) is found to interpret the mechanisms of the motion errors.

References

[1] Z. Wang, Y. Liu and F. Wang, Rapid calculation method for estimating static and dynamic performances of closed hydrostatic guideways, Industrial Lubrication and Tribology, 69 (6) (2017) 1040-1048.

[2] J. Hwang et al., A three-probe system for measuring the parallelism and straightness of a pair of rails for ultra-precision guideways, International J. of Machine Tools and Manufacture, 47 (7-8) (2007) 1053-1058.

[3] Y. Kang et al., Modified predictions of restriction coefficient and flow resistance for membrane-type restrictors in hydrostatic bearing by using regression, Tribology International, 40 (9) (2007) 1369-1380.

[4] J. Zha, F. Xue and Y. Chen, Straightness error modeling and compensation for gantry type open hydrostatic guideways in grinding machine, International J. of Machine Tools and Manufacture, 112 (2017) 1-6.

[5] F. Xue et al., Research on error averaging effect of hydrostatic guideways, Precision Engineering, 36 (1) (2012) 84-90.

[6] Z. Wang et al., Prediction of the effect of speed on motion errors in hydrostatic guideways, International J. of Machine Tools and Manufacture, 64 (2013) 78-84.

[7] P. Zhang et al., Influence of geometric errors of guide rails and table on motion errors of hydrostatic guideways under quasi-static condition, International J. of Machine Tools and Manufacture, 125 (2018) 55-67.

[8] E. Shamoto, C. H. Park and T. Moriwaki, Analysis and improvement of motion accuracy of hydrostatic feed table, CIRP Annals, 50 (1) (2001) 285-290.

[9] J. Zha et al., Motion straightness of hydrostatic guideways considering the ratio of pad center spacing to guide rail profile error wavelength, The International J. of Advanced Manufacturing Technology, 82 (9-12) (2016) 2065-2073.

[10] G. Khim, J. S. Oh and C. H. Park, Analysis of 5-DOF motion errors influenced by the guide rails of an aerostatic linear motion stage, International J. of Precision Engineering and Manufacturing, 15 (2) (2014) 283-290.

[11] W. B. Rowe, Hydrostatic and Hybrid Bearing Design, 1st ed., Butterworth, London, UK (1983).

[12] D. Gao, D. Zheng and Z. Zhang, Theoretical analysis and numerical simulation of the static and dynamic characteristics of hydrostatic guides based on progressive mengen flow controller, Chinese J. of Mechanical Engineering, 23 (6) (2010) 709-716.

[13] S. Yang et al., Hydrostatic worktable performance of an ultra-precision optical aspheric machine tool, Procedia CIRP, 27 (2015) 187-191.

[14] L. Chen et al., Influence of parameters of PM controller on vibration performance of liquid hydrostatic guide-way system, Noise & Vibration Worldwide, 49 (4) (2018) 140-146.

[15] D. Gao et al., Research on the influence of PM controller parameters on the performance of hydrostatic slide for NC machine tool, J. of Mechanical Engineering, 47 (18) (2011) 186-194. (in chinese)

[16] C. Shi et al., Influence of relative difference between paired guide rails on motion accuracy in closed hydrostatic guideways, J. of Mechanical Science and Technology, 34 (2) (2020) 631-648.